A SUPERHYDROPHOBIC NANOFIBER MEMBRANE AND ITS APPLICATION TO DYE FILTRATION USING MEMBRANE DISTILLATION

by

Lei ZHAO[a,b,c], Qianwen WANG[a], Li WEI[a*], Ting ZHU[a], and Jumei ZHAO[a]

[a] Textile and Clothing College, Yancheng Polytechnic College, Yancheng, China
[b] College of Textile and Clothing Engineering, Soochow University, Suzhou, China
[c] National Engineering Laboratory for Modern Silk, Soochow University, Suzhou, China

Original scientific paper
https://doi.org/10.2298/TSCI2403241Z

Direct contact membrane distillation tests are carried out on four kinds of dye solutions using the superhydrophobic polyvinylidene difluron-copolymerized hexafluoropropylene nanofiber membrane (PH-E) and its modification coated with polydimethylsiloxane (PDMS) nanoparticles (PDMS-PH-E membrane). The test results show that PDMS-PH-E membrane has higher water flux, and the removal efficiency of four dyes reaches 100%. While the removal efficiency of the PH-E membrane reaches 100% only for two dyes. The loosely absorbed dye structure on PDMS-PH-E membrane roughens the surface, and stimulates the negatively charged droplets to bounce, resulting in an effective anti-fouling and self-cleaning effect and a long-term scaling prevention.

Key words: *superhydrophobic, nanofiber membrane, membrane distillation, dye solution, Wastewater treatment*

Introduction

The membrane distillation (MD) technology [1] is to use a hydrophobic porous membrane to separate the vapor molecules from wastewater. Due to the temperature difference through the membrane, it is also called a thermally-driven separation process, and it is widely used for dye wastewater treatment [2, 3]. The porous membrane has some amazing thermal properties as discussed in [4-7].

During fabrication of MD membranes, nano/micron particles or organic/inorganic materials are incorporated in the membrane to improve its separation performance. Though the composite MD membranes [8] were recognized for their high functionality and selectivity in a variety of water treatment, the complexity of the chemical method for preparing composite membranes has greatly hindered the practical applications.

In this paper, the well-known bubble electrospinning [9-15] is modified to a bubble electrostatic spraying to control the interface surface by adjusting the inorganic nanomaterials and polymer matrix, the obtained membrane has high porosity and good hydrophobicity, so it can be used as an effective MD membrane. The superhydrophobic polyvinylidene diflourethylene copolymer-hexafluoropropylene (PVDF-HFP) nanofiber membrane (PH-E membrane) was prepared by a modified electrospinning technology with long and spiral needle,

* Corresponding author, e-mail: 170496561@qq.com

which is inspired by the macromolecular electrospinning [16-20] and the multiple needle electrospinning [21]. The bubble electrostatic spraying technology is then used to spray polydimethylsiloxane (PDMS) polymer microspheres onto the PH-E membrane, and the resultant membrane is called as PDMS-PH-E membrane. Both membranes are used for the membrane distillation using four dyes to study their dye removal efficiency.

Materials and methods

The PVDF-HFP were purchased from Zhejiang Juhua Co., LTD., polydimethylsiloxane (PDMS) (basic adhesive, curing agent) was Dow Corning 184, LiCl (analytical pure) was bought from Tianjin Xidan Chemical Technology Co., Ltd., DMF (analytical pure), acetone (analytical pure) and THF (analytical pure) were all provided by Shanghai Runjie Chemical Reagent Co., LTD. Four dyes, methylene blue (MB), crystal violet (CV), acid Red 18 (AR18) and acid yellow 36 (AY36), were supplied by Suzhou City Along Chemical Co., Ltd.

The experiment adopted a modified electrospinning with a 150 mm long needle and a 13 spirals needle, the double needle system was developed from the macromolecular electrospinning using a long needle [16-20], the polyvinylidene fluoride and polyhexafluoropropylene (PVDF-HFP, PH for short) solution was used for fabrication of the superhydrophobic PH-E membrane, which was further treated by the bubble electrostatic spraying, a layer of spherical polymer microspheres was spayed onto the surface of the PH-E membrane, and the PDMS-PH-E membrane was obtained. In the electrospinning process, LiCl accounted for 0.8% of the spun solution, the mass ratio of PH:DMF: acetone was 15:59.5:25.5, the high voltage electrostatic was 20 kV, the receipt distance was 16 cm, the flow rate of injection pump was 0.75 mL per hours, and the spinning period was 10 hours. In the bubble electrostatic spraying process, the mass ratio of the precursor to PDMS solution was 10:1, the mass ratio of DMF to THF was 1:1, the mass ratio of PDMS, PVDF and (DMF/THF) was 2.5:2.5:95, the high voltage static voltage was 30 kV, and the spraying distance was 12 cm.

A SEM JMS - IT100 (Japanese electronics co., LTD) was used to observe the surface morphology of the original membranes and polluted membranes, respectively, the wettability of the membrane surface was characterized by the contact angle (CA), the zeta potentiometer (BeNano90) was used to measure the zeta potential (ZP) on the membrane surface.

A self-designed MD membrane was used for the direct contact membrane distillation (DCMD) for dyes wastewater treatment. The initial volumes of the dye solution (dye: 100 mg per L) and the deionized water were 2.0 L and 0.5 L, respectively. The temperature difference was 40 ℃.

To reduce heat loss and temperature fluctuation, a heating plate/agitator and a heat exchanger equipped with a cooler were used to keep the temperature of each solution with a deviation of ±1.5 °C, all pipes were insulated, and the dye solution and the deionized water flowed into the membrane assembly with the flow ratio of 0.5 Lpm with an effective area of 9.8 cm^2.

The pure water flux, *LMH* [Lm^{-2} per hour] can be calculated by:

$$LMH = \frac{V}{A_m t} \tag{1}$$

where V is the volume of water vapor passing through the membrane, A_m – the effective area, and t – the time.

The spectrophotometer (UV-2600, SHIMADZU, Japan) was used to measure the dye concentration based on different UV-Visible (UV-vis) wavelengths. The absorbance of four standard solutions with different concentrations was measured at wavelengths 445 nm (for AY36 dye), 508 nm (for AR18 dye), 595 nm (for CV dye) and 660 nm (for MB dye). Dye retention rate, R [%] can be calculated by:

$$R = \left(1 - D\frac{\rho_p}{\rho_f}\right) \times 100\% \tag{2}$$

where ρ_f [mgL^{-1}] is the initial dye concentration, ρ_p [mgL^{-1}] – the final dye concentration, and D – the dilution factor.

The properties of nanofiber membranes related to dye concentration were characterized according to the membrane contamination factor (FF):

$$FF = \left(1 - \frac{J}{J_0}\right) \times 100 \tag{3}$$

where the standard flux (J/J_0) is the membrane flux in 24 hours divided by the pure water flux.

The dye adsorption R_L is calculated by:

$$R_L = \frac{1}{1 + bC_0} \tag{4}$$

where b is Langmuir constant and C_0 – the initial dye concentration. The relationship between FF and initial dye concentration, C_0, is used to determine b and the maximum FF (FFmax) according to:

$$\frac{C}{FF} = \frac{1}{FF_{\max}}C_0 + \frac{1}{FF_{\max}b} \tag{5}$$

We assume that the dye repulsion efficiency is close to 100% and the feeding concentration remains constant.

Results and discussion

Zeta potential of the nanofiber membrane surface

Zeta potential (ZP) [22] is a terminology to describe the electrokinetic potential, which has a major effect on the various properties of nanofiber membranes. The ZP can be considered as the charge of the nanoparticles with respect to the surrounding condition, however, it is not an actual measurement of the surface charge of a single molecule, rather it is a measurement of the double layers of electricity produced by the surrounding ions (*i.e.*, counterbalance ions) in solution. The zeta potential diagram of PH-E membrane and PDMS-PH-E membrane is shown in fig. 1. It can be seen from fig. 1 that both membranes showed negative zeta potential within the tested pH range, and at pH 7.0, PDMS-PH-E membrane has a negative 70 mV ZP.

The MD membrane performance for dye removal

The PDMS-PH-E membrane has the lowest wettability with a contact angle as large as 156.2°, so it is suitable for a MD membrane. It was reported that the nanofiber membrane

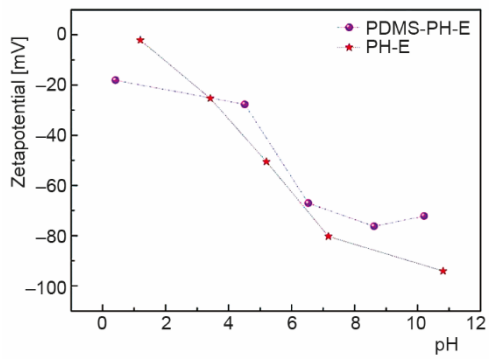

Figure 1. The ZP of PH-E membrane and PDMS-PH-E membrane *vs.* pH value

wetting property can be controlled by nanofibers morphology [23-26] and can be explained by the geometrical potential theory [27]. Four different dyes were treated using PH-E membranes and PDMS-PH-E membranes, the feed temperature was 60 °C, the flow rate was 0.5 Lpm, and the initial dye concentration was 100 mg/L.

The MD water flux

Compared with PH-E membrane, PDMS-PH-E membrane has higher porosity and better hydrophobicity, resulting in higher flux. As shown in fig. 2, the initial fluxes of PH-E membrane and PDMS-PH-E membrane were almost same (about 32 L/m^2 per hour), and the water flux decreases rapidly within 8 hours. When treated for more than 8 hours, the water flux of the two membranes tended to be stable. In addition, the PH-E membrane saw the highest water flux of the AY36 dye, and the lowest water flux was the CV dye. The decreasing order of dye flux was AY36 > AR18 > MB > CV. The PDMS-PH-E membrane saw the highest water flux of the AR18 dye, and the lowest water flux was also observed in the CV dye, the decreasing order of dye wastewater flux followed: AR18 >AY36 > MB > CV.

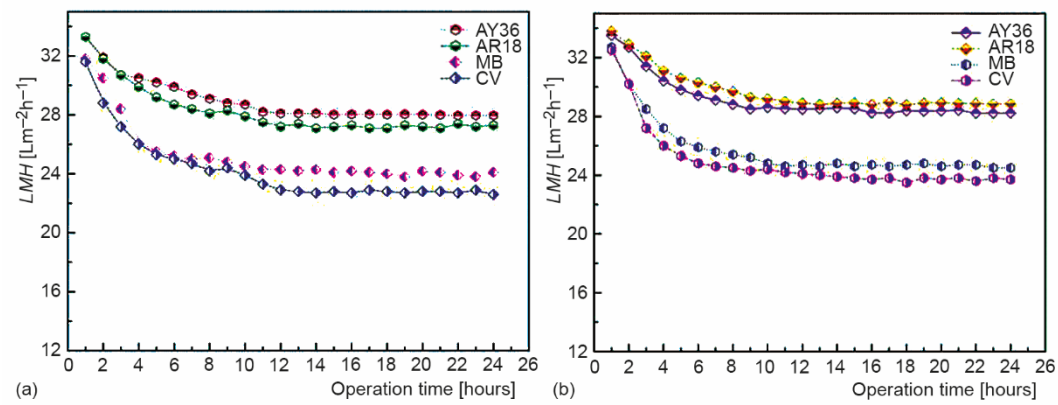

Figure 2. The relationship between the water fluxes of four different dyes during the DCMD treatment with respect to time; (a) PH-E membrane and (b) PDMS-PH-E membrane

Dye removal and its mechanism

As shown in tab. 1, compared with PH-E membrane, PDMS-PH-E membrane has higher water flux, and the dye removal of PDMS-PH-E membrane is superior to other membranes within 24 hours of treatment. Both membranes are conducive to dye removal of AR18 and AR36 dyes (100%), while it is difficult for PH-E membrane to completely remove MB and CV dyes. The removal efficiency of the MB dye is slightly higher than that of the CV dye in DCMD treatment with PH-E membrane. We found that the membrane with higher flux shows higher dye removal efficiency. When PH-E membrane was used for DCMD treatment,

the average flux and dye removal efficiency of MB and CV dyes were 25.31 LMH, 98.76%, and 23.97 LMH, 96.59%, respectively.

Table 1. Initial flux, average flux and dye removal efficiency of four different dyes treated by DCMD within 24 hours

Membrane		MB dye	CV dye	AR18 dye	AR36 dye
PH-E membrane	Initial flux	31.59 ±0.27	31.98 ±0.55	32.82 ±0.45	32.97 ±0.68
	Average flux	25.31 ±1.50	23.97 ±0.91	28.22 ±1.03	29.07 ±0.75
	Dye removal efficiency [%]	98.76 ±0.29	96.59 ±0.94	100	100
PDMS-PH-E membrane	Initial flux	32.61 ±0.57	32.98 ±0.29	33.65 ±0.44	33.21 ±0.79
	Average flux	25.25 ±1.59	24.17 ±1.32	29.47 ±1.01	28.78 ±1.07
	Dye removal efficiency [%]	100	100	100	100

The listed results can be explained by the chemical properties of dyes and their effects on membrane adsorption. The MB and CV dyes contain positively and negatively charged groups. The MB dye is a kind of alkaline cationic dyes, which can be dissociated into cationic and anion Cl^- in aqueous solution. The MB dye can be expressed as Dye^+Cl^-. The CV dye is a direct dye that is water soluble and carries organic compounds that bind to ions and polar sites on the membrane. For the MB dye, there is electrostatic attraction between Dye+ in the MB dye and negatively charged nanofiber membrane. For the CV dye, the negative functional group (ZP = 19.8 mV at pH 4.8, as shown in fig. 1) of the nanofiber membrane forms hydrogen bonds between the electron donor nitrogen atom (–N:). As shown in tab. 1, the AR18 and AY36 dyes have the best removal efficiency because they are acidic dyes with negative charge. When their sulfonate groups approach to the membrane, the sulfonate groups are repelling by the highly negative membrane surface. Relatively few molecules in these two dyes are adsorbed on the membrane surface. However, the two kinds of membranes are mainly negatively charged in the solution equilibrium PH range. The pH values of AR18 and AY36 solutions are 9.0 and 6.5, respectively. In this pH range, the surface charges of PH-E membranes and PDMS-PH-E membranes are highly negative, as shown in fig. 1.

For PDMS-PH-E membrane, when the dye is near the nanofiber membrane surface, dye sulfonate groups were highly rejected by the negative membrane surface, so PDMS-PH-E membrane flux in DCMD showed the highest and the most superior dye removal efficiency. The repulsion between PDMS-PH-E membranes and dye negative ions leads to the formation of dye-dye structures on the surface of the membranes rather than in the pores, and in this respect the superhydrophobicity of PDMS-PH-E membranes also contributes to this phenomenon.

Scaling factor and dye adsorption

Wetting, scaling, and fouling are the main properties for membrane distillation [28]. Scaling in DCMD is particularly important because it increases the cost of energy consumption, downtime, cleaning and membrane replacement, and reduces the quality of the product (water) due to pore wetting. Dye removal, attraction, and repulsion between dyes and mem-

branes depend on their chemical structure and interactions, suggesting that chemical bonding plays an important role in dye contamination during DCMD operation. To elucidate scaling during MD treatment, the membranes were removed after 24 hours of the CV dye treatment, and their scaling surfaces were analyzed using SEM. As shown in fig. 3, sheet crystals cover the surface of PDMS-PH-E membrane, but the pores remain open. However, the dye molecules block a large number of pores in the PH-E membrane. Careful observation shows that the loosely absorbed dye structure on the PDMS-PH-E membrane roughens the surface to stimulate the negatively charged droplets to bounce, thus producing effective anti-fouling and self-cleaning effects [29].

In order to further understand the mechanism of membrane contamination by dye concentration during DCMD operation, the MB solution with different concentrations (20-200 ppm) was treated with two membranes and DCMD technique. We found that the flux was the same at the beginning regardless of the dye concentration, but a larger decline was observed at higher dye concentrations shortly thereafter, and for both membranes the flux was basically stable over 24 hours when the dye concentration was lower (20-40 ppm). In contrast, at dye concentrations higher than 60 ppm (up to 200 ppm), a rapid decline in flux occurs during the first 4-8 hours of operation.

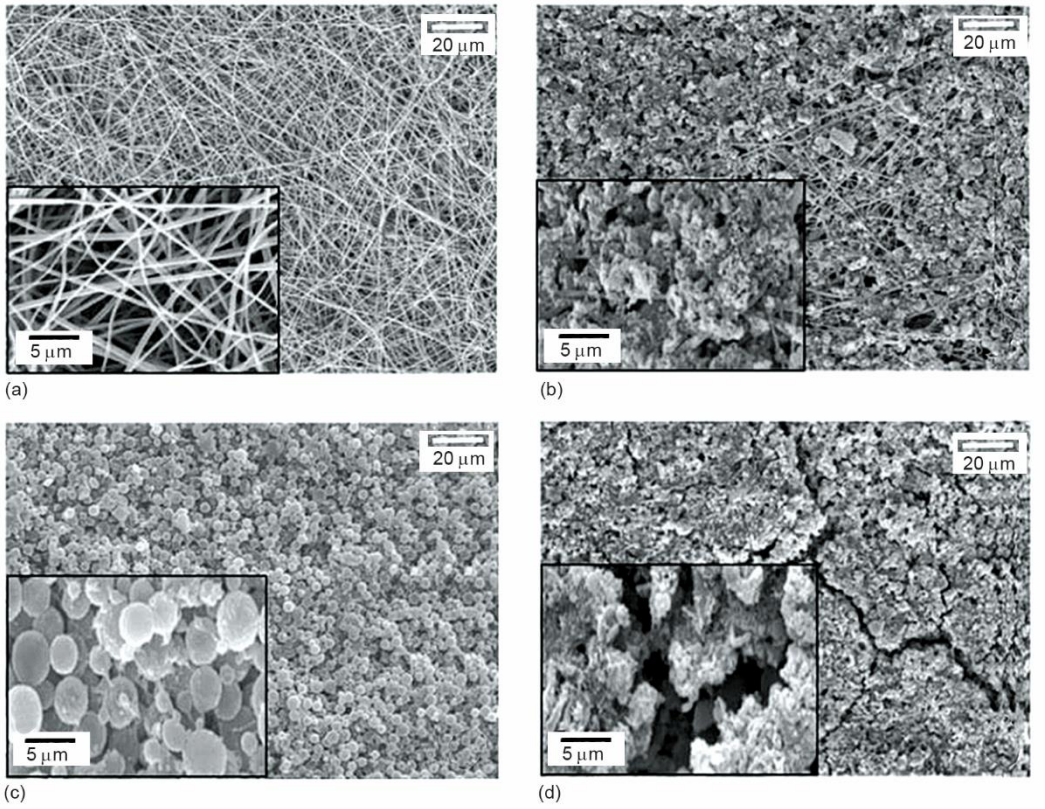

Figure 3. The SEM images; (a) original PH-E membrane, (b) PH-E membrane after DCMD, (c) original PDMS-PH-E membrane, and (d) PDMS-PH-E membrane after DCMD

Figure 4 shows the relationship between the membrane contamination factor, *FF*, and dye concentration in MB treated by DCMD technology within 24 hours. With the increase of dye concentration, *FF* remains constant when it is below 40 ppm, rapidly increases from 40 ppm to 100 ppm, and then becomes basically stable when it is above 100 ppm. The rapid increase in dye concentration between 40 and 100 ppm is mainly attributed to pore blocking and concentration differential polarization caused by dye adsorption. The relationship between *FF* and initial dye concentration, C_0, was used to determine *b* and *FF*max.

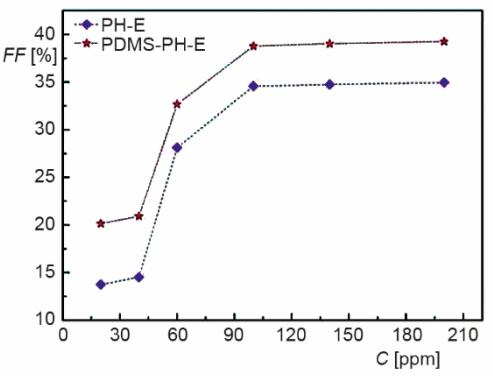

Figure 4. The relationship between dye concentration and the membrane contamination factor treated by DCMD technique within 24 hours

The *FF*max and *b* of PH-E membrane were 45.66% and 0.019 mg/L, respectively, and 46.08% and 0.036 mg/L, respectively, for PDMS-PH-E membrane. The dye adsorption, R_L, for PH-E membranes ranged from 0.73 to 0.21, and from 0.58 to 0.12 for PDMS-PH-E membranes. Absorption is favorable at $0 < R_L < 1$, and it can be said that both membranes exhibit good dye absorption.

Self-cleaning performance of superhydrophobic membrane surface

The surface of PDMS-PH-E membrane has an uneven superhydrophobic surface and is decorated with convolutional microspheres, which generate a bouncing mechanism between the liquid dye droplets and the membrane surface, thus inducing the dye to roll off instead of adhering to the surface, thus improving the antifouling performance. A simple deionized water washing (WF) MD membrane was used, and the CA and liquid entry pressure (LEP) values before and after the membrane were compared to prove the cleaning efficiency of the membrane.

The MD cleaning was carried out at a flow rate of 0.5 Lpm, and the deionized water was circulated every three hours for 10 minutes. After MD operation, CA and LEP of PDMS-PH-E membrane decreased, but WF recovered after only 10 minutes, as shown in fig. 5. However, CA and LEP cannot be fully recovered with WF after MD manipulation of the PH-E membrane because the membrane has a stronger adhesion to water droplets on the surface than PDMS-PH-E membrane. These results indicate that the WF technique has the ability to prevent long-term scaling during MD operations using PDMS-PH-E membranes. In addition, during MD operation for 24 hours, because CV is the most difficult dye to remove dye, the CV dye solution was taken as the re-

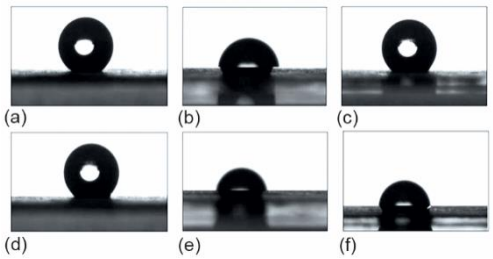

Figure 5. Contact angles of PDMS-PH-E and PH-E membranes; (a) the original PDMS-PH-E membrane, (b) after 24 h MD operation, (c) PDMS-PH-E membrane (24 hours after MD operation and washed for 10 minutes), (d) the original membrane of PH-E membrane, (e) PH-E membrane after 24 hours of MD operation, and (f) PH-E membrane (after 24 hours of MD operation and washed for 10 minutes.

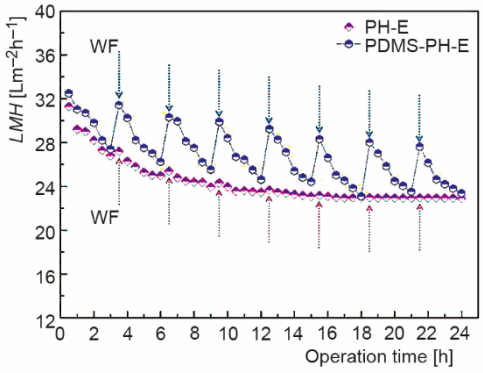

Figure 6. Relation between the water flux of PH-E and PDMS-PH-E membranes in CV treatment (C_0 = 110 mg/L) and the MD operation time (after 3 hours of MD, the membranes were washed with water at 0.5 Lpm flow rate for 10 minutes)

Figure 7. Surface photos of periodic WF membranes for CV dye solution treated by DCMD for 24 hours; (a) PH-E membrane and (b) PDMS-PH-E membrane

search object to test the effect of WF on dirt removal and flux recovery, as shown in fig. 6. During MD operation, PDMS-PH-E membrane showed high flux recovery. This is obviously because PDMS-PH-E membrane has a greater recovery of CA after WF.

The flux of PDMS-PH-E membrane was mainly recovered because of WF. The droplet bouncing caused by superhydrophobicity and the characteristic morphology of PDMS microspheres prevented dye particles from entering the pore and accumulating on the surface. Loose fouling layer was formed on PDMS-PH-E membrane for the reasons that the binding force between dye and membrane was weak, there was a repulsion strength between dye molecules and functional groups on PDMS-PH-E membrane, and the fluffy dye structure was formed before the dye molecules enter the pores. Therefore, the dye fouling layer on PDMS-PH-E membrane can be easily removed by WF. The results confirmed that the superhydrophobicity of the membranes was one of the most critical factors in determining their anti-wetting and anti-fouling properties as well as dye removal efficiency. During the DCMD operation, the two membranes were cleaned with WF, and it was observed that the surface of DMS-PH-E membrane was relatively clean, while the PH-E membrane showed severe dye adsorption and turned into a deep purple nanofiber membrane surface, fig. 7.

Conclusion

The PDMS-PH-E membrane has a loose dye structure resulting in surface roughness, which will greatly affect the boundary layer of the porous membrane [30-33], as a result the surface has an effective anti-fouling and self-cleaning effect, PDMS-PH-E membrane has the ability to prevent long-term scaling during the DCMD operation of WF. Therefore, the PDMS-PH-E membrane developed in this study will also have a huge application capacity in the desalination of seawater, medical wastewater DCMD treatment and other industries.

Acknowledgment

This research was funded by Jiangsu Higher Vocational College Teachers' Professional Leaders' High and Training Team Visit Project (Grant number: 2022TDFX008), Qing Lan Project of Jiangsu Colleges and Universities for Excellent Teaching Team in 2023 (Letter from the Faculty Department of Jiangsu Provincial Department of Education, 2023, No. 27) and Scientific Research Fund of Yancheng Polytechnic College (ygy2302), Jiangsu Province

Higher Vocational Education High-level Major Group Construction Project-Modern Textile Technology Major Group (Grant number: Jiangsu Vocational Education 2020. No 31), Brand Major Construction Project of International Talent Training in Colleges and Universities-Modern Textile Technology Major (Grant number: Jiangsu Foreign Cooperation Exchange Education 2022. No 12), and Key technology innovation platform for flame retardant fiber and functional textiles in Jiangsu Province (2022JMRH-003) all supported this research.

References

[1] Alkhudhiri, A., *et al*., Membrane Distillation: A Comprehensive Review, *Desalination, 287* (2012), Feb., pp. 2-18
[2] An, A. K., *et al*., PDMS/PVDF Hybrid Electrospun Membrane with Superhydrophobic Property and Drop Impact Dynamics for Dyeing Wastewater Treatment Using Membrane Distillation, *Journal of Membrane Science, 525* (2017), Mar., pp. 57-67
[3] Al-salmi, M., *et al*., Application of Membrane Distillation for the Treatment of Oil Field Produced Water, *Desalination, 494* (2020), 114678
[4] Liu, F. J., *et al*., Thermal Oscillation Arising in a Heat Shock of a Porous Hierarchy and Its Application, *Facta Universitatis Series: Mechanical Engineering*, *20* (2022), 3, pp. 633-645
[5] He, C. H., *et al*., A Fractal Model for the Internal Temperature Response of a Porous Concrete, *Applied and Computational Mathematics, 21* (2022), 1, pp. 71-77
[6] Nadeem, M., *et al*., Chemical Reaction and Radiation on the Boundary-Layer Flow of Electrically Conduction Micropolar Fluid Through a Porous Shrinking Sheet, *Thermal Science, 26* (2022), 3B, pp. 2593-2598
[7] Ain, Q. T., *et al*., An Analysis of Time-Fractional Heat Transfer Problem Using Two-Scale Approach, *GEM-International Journal on Geomathematics, 12* (2021), 18, pp. 1-10
[8] Wang, K. P., *et al*., Development of a Composite Membrane with Underwater-Oleophobic Fibrous Surface for Robust Anti-Oil-Fouling Membrane Distillation, *Journal of Colloid and Interface Science*, *537* (2019), Mar., pp. 375-383
[9] He. J. H., *et al*., BioMimic Fabrication of Electrospun Nanofibers with High-Throughput, *Chaos, Solitons and Fractals, 37* (2008), 3, pp. 643-651
[10] He, J. H., *et al*., The Maximal Wrinkle Angle During the Bubble Collapse and Its Application to the Bubble Electrospinning, *Frontiers in Materials*, 8*(* 2022), 800567
[11] Qian, M. Y., He, J. H., Collection of Polymer Bubble as a Nanoscale Membrane, *Surfaces and Interface, 28* (2022), 101665
[12] He, C. H., *et al*., Taylor Series Solution for Fractal Bratu-type Equation Arising in Electrospinning Process, *Fractals, 28* (2020), 1, 2050011
[13] Li, X. X., He, J. H., Bubble Electrospinning with an Auxiliary Electrode and an Auxiliary Air Flow, *Recent Patents on Nanotechnology, 14* (2020), 1, pp. 42-45
[14] He, J. H., *et al*., Review on Fiber Morphology Obtained by Bubble Electrospinning and Blown Bubble Spinning, *Thermal Science, 16* (2012), 5, pp. 1263-1279
[15] Zuo, Y. T., Liu, H. J., Effect of Temperature on the Bubble Electrospinning Process and Its Hints for 3-D Printing Technology, *Thermal Science, 26* (2022), 3B, pp. 2499-2503
[16] Tian, D., He, J. H., Self-Assemble of Macromolecules in a Long and Narrow Tube, *Thermal Science, 22* (2018), 4, pp. 1659-1664
[17] Tian, D., He, J. H., Macromolecular Electrospinning: Basic Concept & Preliminary Experiment, *Results in Physics, 11* (2018), Dec., pp. 740-742
[18] Tian, D., *et al*., Macromolecule Orientation in Nanofibers, *Nanomaterials*, *8* (2018), 11, 918
[19] Tian, D., He, J. H., Macromolecular-Scale Electrospinning: Controlling Inner Topologic Structure Through a Blowing Air, *Thermal Science, 26* (2022), 3B, pp. 2663-2666
[20] Tian, D., *et al*., Macromolecule's Orientation in a Nanofiber by Bubble Electrospinning, *FDMP-Fluid Dynamics & Materials Processing, 17* (2021), 4, pp. 711-720
[21] Li, X. X., *et al*., Multiple Needle Electrospinning for Fabricating Composite Nanofibers with Hierarchical Structure, *Journal of Donghua University (English Edition), 38* (2021), 1, pp. 63-67
[22] Honary, S., Zahir, F., Effect of Zeta Potential on the Properties of Nano-Drug Delivery Systems – A Review (Part 1), *Tropical Journal of Pharmaceutical Research, 12* (2013), 2, pp. 255-264

[23] Li, X. X., *et al*., High Energy Surface as a Receptor in Electrospinning: A Good Switch for Hydrophobicity to Hydrophilicity, *Thermal Science*, *25* (2021), 3B, pp. 2205-2212
[24] Liu, L. G., *et al*., Dropping in Electrospinning Process: A General Strategy for Fabrication of Microspheres, *Thermal Science*, *25* (2021), 2B, pp. 1295-1303
[25] Peng, N. B., He, J. H., Insight into the Wetting Property of a Nanofiber Membrane by the Geometrical Potential, *Recent Patents on Nanotechnology*, *14* (2020), 1, pp. 64-70
[26] Li, X. X., *et al*., Boosting Piezoelectric and Triboelectric Effects of PVDF Nanofiber Through Carbon-Coated Piezoelectric Nanoparticles for Highly Sensitive Wearable Sensors, *Chemical Engineering Journal*, *426* (2021), 130345
[27] Peng, N. B., He, J. H., Insight into the Wetting Property of a Nanofiber Membrane by the Geometrical Potential, *Recent Patents on Nanotechnology*, *14* (2020), 1, pp. 64-70
[28] Warsinger, D. M., *et al*., Scaling and Fouling in Membrane Distillation for Desalination Applications: A Review, *Desalination*, *356* (2015), Jan., pp. 294-313
[29] Han, C. Y., He, J. H., Effect of Fabric Surface's Cleanliness on Its Moisture/Air Permeability, *Thermal Science*, *25* (2021), 2B, pp. 1517-1521
[30] He, J. H., Elazem, N. Y. A., The Carbon Nanotube-Embedded Boundary Layer Theory for Energy Harvesting, *Facta Universitatis Series: Mechanical Engineering*, *20* (2022), 2, pp. 211-235
[31] Kou, S. J., *et al*., Fractal Boundary Layer and Its Basic Properties, *Fractals*, *30* (2022), 9, 22501729
[32] Mei, Y., *et al*., On the Mountain-River-Desert Relation, *Thermal Science*, *25* (2021), 6B, pp. 4817-4822
[33] Kumar, K., *et al*., Irreversibility Analysis in Al_2O_3-Water Nanofluid Flow with Variable Property, *Facta Universitatis Series: Mechanical Engineering*, *20* (2022), 3, pp. 503-518

Paper submitted: April 1, 2023
Paper revised: August 5, 2023
Paper accepted: August 7, 2023